

Evaluating the Impact of Uncertainty on Airport Surface Operations

Sandeep Badrinath* and Hamsa Balakrishnan†
Massachusetts Institute of Technology, Cambridge, MA 02139, USA

Emily Clemons‡ and Tom G. Reynolds §
MIT Lincoln Laboratory, Lexington, MA 02421, USA

Flights spend significantly more time taxiing on the airport surface during periods when the departure demand exceeds airport capacity, resulting in excessive fuel burn. Departure metering by holding aircraft at the gate during periods of congestion has been shown to yield benefits by lowering the taxi-out time. However, an important aspect of this problem that has not been understood well is the impact of uncertainty in departure demand. Recently, some airlines are beginning to publish an expected time that the flights are ready to pushback, which is referred to as Earliest Off-Block Time (EOBT). Tactical decisions for departure metering need to be made with the EOBT information. However, the EOBT published by airlines is often found to deviate from the actual gate out time without departure metering, which represents an error in the EOBT estimate. Hence, it is important to consider errors in EOBT information while analyzing benefits from departure metering.

In this paper, we present a queuing network model to predict aircraft taxi-times on the airport surface. The predictions from the queue model are used for departure metering with NASA's ATD-2 logic that is being used in field trials at Charlotte airport. The framework allows us to quantify the reduction in departure metering benefits due to errors in EOBT information. The analysis reveals that the benefits reduce significantly due to EOBT uncertainty which has important implications for future departure metering applications, such as through the Terminal Flight Data Manager (TFDM) platform.

I. Introduction

GLOBAL passenger air travel demand is expected to double over the next 20 years, accompanied by an increase in the number of operations [1]. However, critical airport infrastructures such as runways that determine the capacity of the airport have not improved significantly to meet the growth in air traffic. Runways and certain taxiways have become bottlenecks at major airports, leading to congestion on the airport surface. The result of congestion is increased travel time for aircraft on the ground.

Predicting the taxi time (travel time of aircraft on the surface) has been an important topic of research in the air traffic community for many reasons. Aircraft surface operations contribute significantly to the emissions at the airport. With concerns over global warming, regulatory agencies have started monitoring emissions from the airport. This has led to a growing interest in predicting emissions on the airport surface in order to monitor them [2]. Aircraft emissions on the surface depends on the amount of fuel burned, which in-turn is proportional to the taxi-time [3]. Industry standard tools to estimate fuel burn and emissions such as the FAA's Aviation Environmental Design Tool (AEDT) rely on good estimates of taxi time [2, 4].

Taxi time models also enable tactical scheduling decisions to reduce congestion on the airport surface. Currently, ramp controllers provide clearance for departures to pushback from the gate whenever the pilots call ready. A well

*Graduate student, Department of Aeronautics and Astronautics, Massachusetts Institute of Technology. AIAA member

†Associate Professor, Department of Aeronautics and Astronautics, Massachusetts Institute of Technology. AIAA Associate Fellow.

‡Assistant Staff, Air Traffic Control Systems Group.

§Associate Group Leader, Air Traffic Control Systems Group. AIAA Associate Fellow

DISTRIBUTION STATEMENT A. Approved for public release: distribution unlimited. This material is based upon work supported by the Federal Aviation Administration under Air Force Contract No. FA8721-05-C-0002 and/or FA8702-15-D-0001. Any opinions, findings, conclusions or recommendations expressed in this material are those of the author(s) and do not necessarily reflect the views of the Federal Aviation Administration.

known strategy that has been demonstrated to reduce congestion on the airport surface is to hold departures at the gate during periods of congestion and release them appropriately when there is reduced congestion [5–7]. Holding aircraft at the gate with their engines turned off results in fuel and emissions savings, however, it is equally important to release the held aircraft at the right time so that the runway is not under-utilized. Recent efforts by NASA through the Airspace Technology Demonstration (ATD-2) program at Charlotte Douglas International airport (CLT) plans to reduce congestion by assigning a holding time for the departures at the gate based on taxi-time prediction [8]. For this strategy to work well, one of the key components is to obtain good predictions for taxi time.

Researchers have previously used different techniques to predict taxi-time: Queuing models, stochastic node-link models, discrete event simulations, and models based on statistical regression [9–12]. From the perspective of controlling pushbacks at the gate, the focus has been on developing models for the departure process. These models typically involved a single queue to represent queuing near the departure runway, and the taxi-out time (time taken for an aircraft to travel from the gate to the runway) was obtained as the sum of the unimpeded time to the runway and wait-time in the queue [9]. At many airports such as CLT, congestion can occur at multiple areas rather than only at the departure queues. Such airports can be modeled by more complex queuing networks [7].

The aforementioned taxi time models all require the actual pushback time as a key input. Therefore, in order to make tactical decisions on holding departures at the gate based on the predicted taxi-out time for future flights, we need an accurate estimate of the pushback time, for example, the Earliest Off-Block Time (EOBT). The actual pushback time or call ready time could differ from the EOBT published by the airlines due to many operational reasons. Since the estimated pushback time might deviate from the EOBT, it becomes important to examine the uncertainty in pushback time given the reported EOBTs. To the best of our knowledge, there has been limited research on the impact of uncertainty in EOBT on surface operations [13]. The main contributions of this paper are as follows,

- A new queuing network model for the airport surface is presented that is capable of predicting taxi-times for departures as well as arrivals.
- Potential benefits of departure metering is determined using NASA’s ATD-2 algorithm with inputs from the queue model.
- Impact of EOBT uncertainty on taxi-out time prediction, as well as the resulting impact on departure metering benefits is examined.

This paper presents analysis with focus on CLT. Section II presents an overview of CLT operations, Section III discusses a queuing model for CLT operations and Section IV discusses departure metering applied to CLT. Section V presents the impact of EOBT uncertainty on CLT departure metering activities. Finally, Section VI discusses conclusions and planned next steps.

II. CLT operations

Handling more than 1,400 commercial operations everyday, CLT is the seventh busiest airport in the world in terms of aircraft movement [14]. Fig. 1(a) shows the airport layout of CLT along with a snapshot of aircraft positions, taxi-out flights (departures) represented by black triangles and taxi-in flights (arrivals) represented by white triangles. Three parallel runways (36L, 36C and 36R) are actively used in this particular configuration (North-flow). All three runways are used for landing, whereas, only 36C and 36R are used for takeoffs. We can clearly see queues being formed in the ramp area, near the runway crossing and departure runways (highlighted in Fig. 1(a)).

Accounting for congestion at multiple areas, the movement of traffic on the airport surface can be best represented as a queuing network shown in Fig. 1(b). The network is comprised of five queues, three for the taxi-out flight movement (shown in blue) and two for the taxi-in flight movement (shown in red). The departures pass through a taxi-out ramp queue and one of the two runway queues depending on their runway assignment. Flights landing on the leftmost runway (36L) pass through a runway crossing queue and taxi-in ramp queue, whereas, flights landing on the other runways just pass through the taxi-in ramp queue. If we can model the queue dynamics, the taxi-time can be estimated as the sum of the unimpeded time (travel time without any delay) and wait time in the queues.

Probabilistic models are generally used to analyze queuing systems [15]. However, a lot of challenges arise in using probabilistic models to represent large queuing networks such as these. A part of the challenge is that these queues are inherently non-stationary due to fluctuating traffic demand and airport capacity. Hence we need a different framework to handle such a queuing network.

In this paper, a new queuing network model for the airport surface is presented that is able to capture congestion in multiple areas. Instead of using a probabilistic model to describe the queuing process, we use a fluid flow model in the present work. The model describes the evolution of queue length as a solution to a simple first order non-linear

differential equation [16] [7]. Although the model is deterministic, it captures the dynamic behaviour of non-stationary queues. The model allows us to predict taxi-times for both arrivals and departures. Using actual operational data from CLT, we show that our queuing model performs very well in terms of predicting the queue sizes on the airport surface as well as the taxi-times.

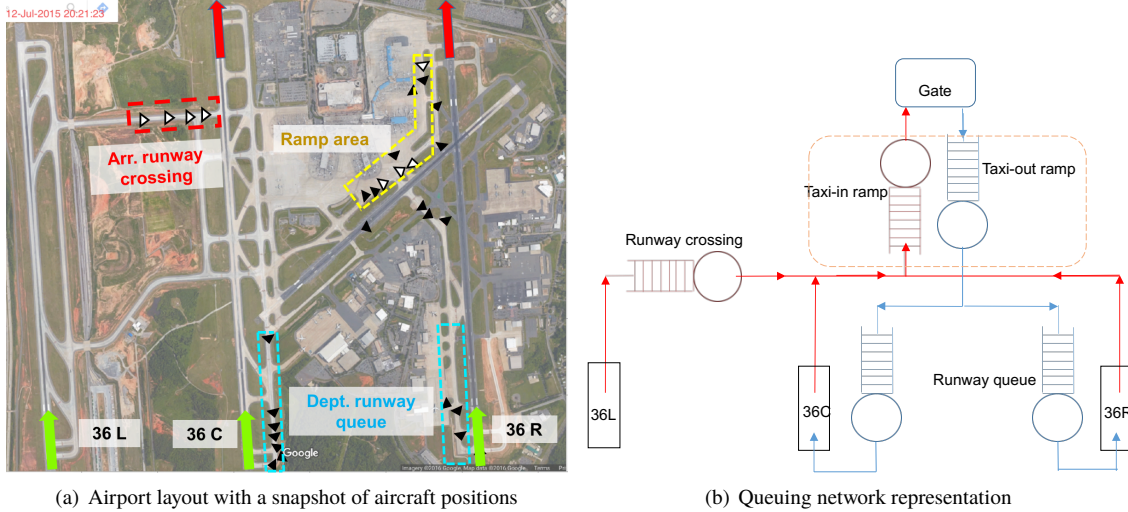


Fig. 1 (a) Airport layout for Charlotte Douglas International airport (CLT). The flights taxiing-in and those taxiing-out are represented by white and black triangles, respectively. The ramp queue and departure runway queue are shown in yellow and cyan, respectively. The taxi-in runway crossing queue is shown in red. Departure runways are indicated with red arrows and arrival runways with green arrows (b) Queuing network model for the airport surface, the taxi-in queues shown in red and taxi-out queues shown in blue.

III. Queuing model for the airport surface

In this section, we model the surface traffic at CLT using a queuing network model. The model is based on the point-wise stationary fluid flow approximation for queues [7, 17].

A. Fluid flow model for non-stationary queues

The fluid model is a continuum approximation to the discrete queuing problem. Let $\lambda(t)$ be the arrival rate into the queue and $\mu(t)$ be the mean service rate of the server. Then the dynamics of the queue length ($x(t)$) is given by the following equation [7],

$$\dot{x}(t) = -\mu(t) \frac{C(t)x(t)}{1 + C(t)x(t)} + \lambda(t) \quad (1)$$

Here, C is a positive parameter that depends on the coefficient of variation of the service time distribution of the server. We can consider the negative term in the above equation (1) as the out-flow rate from queue and $\lambda(t)$ to be the in-flow rate into the queue. Using this idea, we can potentially extend the model to a network of queues.

B. Model for the airport surface

1. Taxi-out process

From the queuing representation of the airport surface (shown earlier in Fig. 1(b)), the taxi-out flights pass through the taxi-out ramp queue and departure runway queue. An aircraft is said to be in the taxi-out ramp queue if its travel time after pushing back from the gate has exceeded the unimpeded gate to spot time and it is yet to exit the ramp area (spots are the exit points in the ramp area leading to the active movement area). The customers (aircraft) in the taxi-out ramp queue are categorised into two classes depending on the runway assignment. Let $x_{d,si}$ be the number of flights

in the ramp queue heading to runway i ($i = 1, 2, 3$ corresponds to runway 36L, 36C and 36R respectively). The ramp queue is served by a single server of mean service rate $\mu_{d,s}$. The fraction of service used by each class of customers (aircraft) is assumed to be proportional to the fraction of customers of that particular class in the queue. The input to the queuing dynamics is the pushback rate ($u_{d,ri}$) at the gate to each runway i . In addition to the waiting time at the queue, the total time taken by a flight to exit the ramp area includes the unimpeded travel time to move from the gate to the spot. The unimpeded time varies for different gate-spot combinations depending on the distance between the gate and spot. However, we consider a weighted average unimpeded time over all gate-spot combinations, with the weights proportional to the frequency of operation. The average unimpeded time from gate to spot is represented by t_1 . The unimpeded travel time leads to delay in the ramp queue dynamics, i.e. if the pushback rate at the gate is $u_{d,ri}(t)$, then the arrival rate into the queue is $u_{d,ri}(t - t_1)$. Considering these effects, the dynamics for the taxi-out ramp queue is given by eqs. (2) to (4).

$$x_{d,s}(t) = x_{d,s2}(t) + x_{d,s3}(t) \quad (2)$$

$$\dot{x}_{d,s2}(t) = -\mu_{d,s}(t) \frac{C_{d,s}(t)x_{d,s2}(t)}{1 + C_{d,s}x_{d,s}(t)} + u_{d,r2}(t - t_1) \quad (3)$$

$$\dot{x}_{d,s3}(t) = -\mu_{d,s}(t) \frac{C_{d,s}(t)x_{d,s3}(t)}{1 + C_{d,s}x_{d,s}(t)} + u_{d,r3}(t - t_1) \quad (4)$$

There are two runway queues that are independent of each other. Let $x_{d,ri}$ be the number of aircraft in the i^{th} runway queue and $\mu_{d,ri}$ be the mean service rate of the departure runway server. An aircraft is said to be in the departure runway queue if its travel time after exiting the ramp has exceeded the unimpeded spot to runway time and it is yet to take-off. The output of the ramp queue is the input to the runway queue delayed by time t_2 . Here t_2 is the average unimpeded time from spot to runway. The equations for the dynamics of the runway queue takes the form,

$$\dot{x}_{d,r2}(t) = -\mu_{d,r2}(t) \frac{C_{d,r2}x_{d,r2}(t)}{1 + C_{d,r2}x_{d,r2}(t)} + \mu_{d,s}(t - t_2) \frac{C_{d,s}(t - t_2)x_{d,s2}(t - t_2)}{1 + C_{d,s}(t - t_2)x_{rp}(t - t_2)} \quad (5)$$

$$\dot{x}_{d,r3}(t) = -\mu_{d,r3}(t) \frac{C_{d,r3}x_{d,r3}(t)}{1 + C_{d,r3}x_{d,r3}(t)} + \mu_{d,s}(t - t_2) \frac{C_{d,s}(t - t_2)x_{d,s3}(t - t_2)}{1 + C_{d,s}(t - t_2)x_{rp}(t - t_2)} \quad (6)$$

2. Taxi-in process

Flights landing on 36L have to pass through a runway crossing queue before entering the ramp area. Let $u_{a,ri}$ be the landing rate (of arrivals) on the i^{th} runway. The inputs to the runway crossing queue is the landing rate on runway 36L, with an associated delay (t_3) accounting for the travel time to reach the runway crossing queue from the point of touchdown. The dynamics for the runway crossing queue length ($x_{a,r1}$) is given by,

$$\dot{x}_{a,r1}(t) = -\mu_{a,r1}(t) \frac{C_{a,r1}x_{a,r1}(t)}{1 + C_{a,r1}x_{a,r1}(t)} + u_{a,r1}(t - t_3) \quad (7)$$

An aircraft is defined to be in the taxi-in ramp queue if it has entered the ramp area and is yet to reach the gate after spending unimpeded spot to gate time in the ramp area. The inputs to the taxi-in ramp queue dynamics is the sum of landing rate on the two runways (36C and 36R) and the output from the runway crossing queue, delayed by the average unimpeded spot to gate time (t_4). We could also account for the travel time from the runway (36C and 36R) to the spot in the delay term. However, we ignore it here since it is a small value but consider it later while computing the taxi-time. The equation for the taxi-in ramp queue length ($x_{a,s}$) is given by,

$$\dot{x}_{a,s}(t) = -\mu_{a,s}(t) \frac{C_{a,s}x_{a,s}(t)}{1 + C_{a,s}x_{a,s}(t)} + \mu_{a,r1}(t) \frac{C_{a,r1}(t - t_4)x_{a,r1}(t - t_4)}{1 + C_{a,r1}(t - t_4)x_{a,r1}(t - t_4)} + u_{a,r2}(t - t_4) + u_{a,r3}(t - t_4) \quad (8)$$

C. Data sources

Operational data for CLT was extracted from multiple sources. The flight tracks on the surface were obtained from airport surface surveillance data (ASDE-X) [18]. The tracks were used to determine the time when an aircraft reached the spot and runway. The actual pushback time, in-air time, landing time, in-gate time and gate assignment were obtained from OAG data [14]. The meteorological condition at the airport (VMC/IMC) was obtained using ASPM data [19]. The dataset contains 27,784 arrivals and 27,117 departures, and around 70% was used to train the model parameters and the rest was used for testing.

D. Server service rates

The service rates for the queue servers are determined from operational data. The service time distribution of the server is obtained by computing the difference between successive out-times from the queue when there is pressure on the server.

1. Ramp queue

Congestion develops in the ramp area primarily because taxi-in and taxi-out flights share some common taxi paths while heading in different directions. The service rate of the taxi-out ramp server is modeled as a function of the queue length of the taxi-in ramp queue and vice-versa. Fig. 2(a) shows the mean service rate of the taxi-in ramp server as a function of the length of the taxi-out ramp queue. We see that the mean service rate of the taxi-in ramp server decreases with increase in number of taxi-out aircraft and follows a linear trend. Similarly, the mean service rate of the taxi-out ramp server was observed to decrease with increase in the number of taxi-in aircraft. A linear fit to the data yields the following relationship for the service rates as a function of the traffic on the ramp,

$$\mu_{d,s}(t) = -0.033x_{a,s}(t) + 1.7 \quad (9)$$

$$\mu_{a,s}(t) = -0.066x_{d,s}(t) + 1.6 \quad (10)$$

The service rate is expressed in terms of aircraft per minute.

2. Departure runway queue

Successive flights using the runway, either takeoffs or landings, need to be sufficiently separated to reduce the effect of wake vortex of the leading aircraft on the trailing aircraft. The separation constraint decides the capacity of the runway. The runway used for takeoffs are also used for landings in CLT, resulting in additional separation requirements. The separation time depends on various factors such as the size of the leading and trailing aircraft using the runway, type of operation of the leading aircraft (landing or take-off), and weather condition at the airport. The effect of aircraft size is not significant here since around 98% of the flights operating from CLT belong to the 'large' category of aircraft weight class. We assume that departure throughput of the runway server in a small time window (5 min) depends only on two factors: (a) the number of landings on that runway in that time window (b) weather condition at the airport (VMC/IMC).

Fig. 2(b) shows the dependence of the mean service rate of the departure runway server as a function of the number of landings on the runway during good weather condition (VMC). We can see that the mean service rate decreases with increase in the number of landings as one would expect. An empirical model of the mean service rate for the two runway servers in different weather conditions is as follows,

$$\mu_{d,r2}(t)|_{VMC} = -0.14n_{a,r2}(t) + 0.82 \quad (11)$$

$$\mu_{d,r3}(t)|_{VMC} = -0.11n_{a,r3}(t) + 0.79 \quad (12)$$

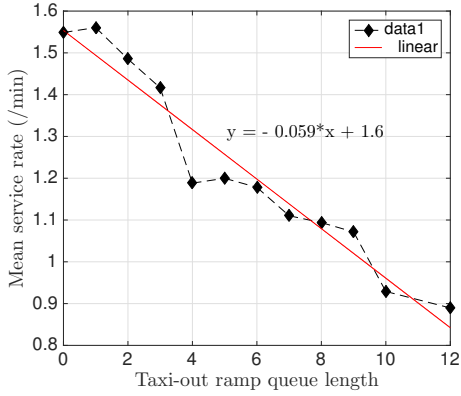
$$\mu_{d,r2}(t)|_{IMC} = -0.14n_{a,r2}(t) + 0.74 \quad (13)$$

$$\mu_{d,r3}(t)|_{IMC} = -0.11n_{a,r3}(t) + 0.77 \quad (14)$$

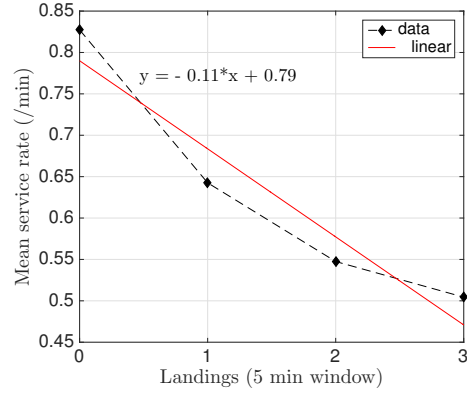
Here, $n_{a,ri}(t)$ denotes the number of landings on runway i in a discrete 5 min time window containing t .

3. Runway crossing queue

The flights that land on runway 36L need to cross runway 36C to reach the ramp area. Flights are not allowed to cross a runway when the runway is being used to handle takeoffs or landings, leading to the formation of a runway crossing queue (shown earlier in Fig. 1(a)). The mean service rate ($\mu_{a,s}$) for runway crossing queue server was found to be 0.96 ac/min.



(a) Mean service rate of taxi-in ramp server as a function of taxi-out ramp queue length



(b) Mean service rate of runway 36R as a function of number of landings in 5 min window (VMC)

Fig. 2 Mean service rate of ramp and runway servers.

E. Coupled surface model

We have modeled the mean service rate of the servers as a function of surface traffic and weather. The coefficient of variation of the service time distributions were found to be independent of traffic, resulting in time independent C_i s. By substituting the expression for mean service rate in eqs. (2) to (8), we obtain the following coupled set of equations for the queuing dynamics,

$$\dot{x}_{d,s2}(t) = -(a_1 x_{a,s}(t) + a_2) \frac{C_{d,s} x_{d,s2}(t)}{1 + C_{d,s} x_{d,s}(t)} + u_{d,r2}(t - t_1) \quad (15)$$

$$\dot{x}_{d,s3}(t) = -(a_1 x_{a,s}(t) + a_2) \frac{C_{d,s} x_{d,s3}(t)}{1 + C_{d,s} x_{d,s}(t)} + u_{d,r3}(t - t_1) \quad (16)$$

$$\dot{x}_{d,r2}(t) = -(a_3 n_{a,r2}(t) + a_4) \frac{C_{d,r2} x_{d,r2}(t)}{1 + C_{d,r2} x_{d,r2}(t)} + (a_1 x_{a,s}(t - t_2) + a_2) \frac{C_{d,s} x_{d,s2}(t - t_2)}{1 + C_{d,s} x_{rp}(t - t_2)} \quad (17)$$

$$\dot{x}_{d,r3}(t) = -(a_5 n_{a,r3}(t) + a_6) \frac{C_{d,r3} x_{d,r3}(t)}{1 + C_{d,r3} x_{d,r3}(t)} + (a_1 x_{a,s}(t - t_2) + a_2) \frac{C_{d,s} x_{d,s3}(t - t_2)}{1 + C_{d,s} x_{rp}(t - t_2)} \quad (18)$$

$$\dot{x}_{a,r1}(t) = -\mu_{a,r1} \frac{C_{a,r1} x_{a,r1}(t)}{1 + C_{a,r1} x_{a,r1}(t)} + u_{a,r1}(t - t_3) \quad (19)$$

$$\dot{x}_{a,s}(t) = -(a_7 x_{d,s}(t) + a_8) \frac{C_{a,s} x_{a,s}(t)}{1 + C_{a,s} x_{a,s}(t)} + \mu_{a,r1} \frac{C_{a,r1} x_{a,r1}(t - t_4)}{1 + C_{a,r1} x_{a,r1}(t - t_4)} + u_{a,r2}(t - t_4) + u_{a,r3}(t - t_4) \quad (20)$$

Here a_i s are constants that depend on the mean service rate of the servers: $a_1 = -0.033$, $a_2 = 1.7$, $a_3 = -0.14$ (VMC), $a_4 = 0.82$ (VMC)/0.74 (IMC), $a_5 = -0.11$, $a_6 = 0.79$ (VMC)/0.77 (IMC), $a_7 = -0.066$, $a_8 = 1.6$.

The inputs to the model are the pushback time, landing time and weather. With appropriate initial conditions, the above delay differential equations can be numerically integrated forward in time to obtain queue length prediction.

F. Taxi-time prediction

The wait times of aircraft entering the queue are determined using queue length predictions and mean service rate predictions. We need to compute the wait time accounting for the fact that the mean service rate can be time varying. Let $x(t_{in})$ be the predicted queue length at time $t = t_{in}$ and let $\mu(t)$ be the mean service rate of the server. The wait

time (W) for an aircraft that entered the queue at t_{in} can be obtained using the following algorithm,

```

 $Q = x(t_{in});$ 
 $q = Q; t = t_{in,i}; W = 0;$ 
while  $q > 0$  do
  |  $q = q - \mu(t)\Delta t;$ 
  |  $W = W + \Delta t;$ 
  |  $t = t + \Delta t;$ 
end
 $W = W + q/\mu(t);$ 

```

Algorithm 1: Computing wait time in a queue

The predicted taxi-time is the sum of unimpeded travel time and wait time in the queues. From the queuing representation of the airport surface, the taxi-out and taxi-in time are given by,

$$T_{out} = t_{u,gs} + W_{d,s} + t_{u,sr} + W_{d,rw} \quad (21)$$

$$T_{in} = t_{u,rs} + W_{cross} + t_{u,sg} + W_{a,s} \quad (22)$$

Here, T_{out} is the predicted taxi-out time, T_{in} is the predicted taxi-in time, $t_{u,gs}$ is the unimpeded gate to spot time, $W_{d,s}$ is the wait time in the ramp queue for taxi-out flights, $W_{d,rw}$ is the wait time in the departure runway queue, $t_{u,rs}$ is the unimpeded travel time for taxi-in flights from runway to spot, W_{cross} is the wait time in the runway crossing queue, $t_{u,sg}$ is the unimpeded spot to gate time for taxi-in flights and $W_{a,s}$ is the wait time in the ramp queue for taxi-in flights. For taxi-in flights, W_{cross} is applicable only for flights landing on 36L. Also note that the unimpeded times are different for different gate-spot and spot-runway combinations unlike the average unimpeded time used in the queuing dynamics. The reason for using an average quantity in the queuing dynamics was to have a constant delay term in the equations. However, to obtain taxi-time for any given flight, one can use flight specific details such as its gate, spot and runway to obtain a better estimate of its unimpeded travel time rather than using an average quantity.

G. Predictive performance of the model

A test set comprising of 7,484 departures and 8,477 arrivals was used to evaluate the model performance. Actual pushback time, landing time and weather condition that are required as inputs to the model were obtained from historical data. The pushback time and landing time are converted into pushback rate ($u_{d,i}(t)$) and landing rate ($u_{a,i}(t)$), that are the actual inputs entering into the queuing equations. The pushback time conditioned on the runway assignment of flights are binned into 5 min windows for the entire day. An average rate is determined for each window that serves as the pushback rate over that particular window. The landing rate is computed in a similar way. The queuing dynamics, eqs. (15) to (20), are numerically integrated forward in time from the beginning of the day with a time discretization of 1 min. The taxi-time is determined after computing the queue lengths.

We first present the queue length and taxi-time predictions for a typical day in the test set that has VMC conditions (Jun 25, 2016). Fig. 3 shows the queue length prediction for the taxi-out ramp queue and departure runway queues. The queue length shown in the plot is the averaged queue length over 1 min window. Overall, we see a good match between the model predictions and data. The prediction errors are comparatively higher for the ramp queue when compared to the runway queue. This is expected since there is more unpredictability in the ramp area. In our model, we have assumed a single server for the ramp queue since majority of the flights use a single spot to exit the ramp. The prediction errors could be large during situations where flights consistently use more than one spot.

A comparison of the queue length for taxi-in flights between the model and data for the same test day is shown in Fig. 4. Even here, we see a reasonable agreement between the model and data, considering the fact that there could be a lot of variability in operational procedures for handling runway crossing. The prediction errors for taxi-in ramp queue arise because of a similar reason that we had mentioned for the taxi-out ramp queue.

Fig. 5 shows the predicted average taxi-out time along with the actual data. Each data point corresponds to an averaging over a 15 min window. The predictions are close to the actual values with the exception of a few points. One can notice that the large errors in the taxi-out time prediction corresponds to time intervals wherein there are errors in the queue length prediction. A similar behaviour can be seen for the taxi-in predictions shown in Fig. 4.

The error statistics for taxi-out time predictions over 7,484 flights in the test set is shown in Table 1. In addition to the errors in total taxi-out time, the table also contains information about errors in gate to spot time and spot to runway

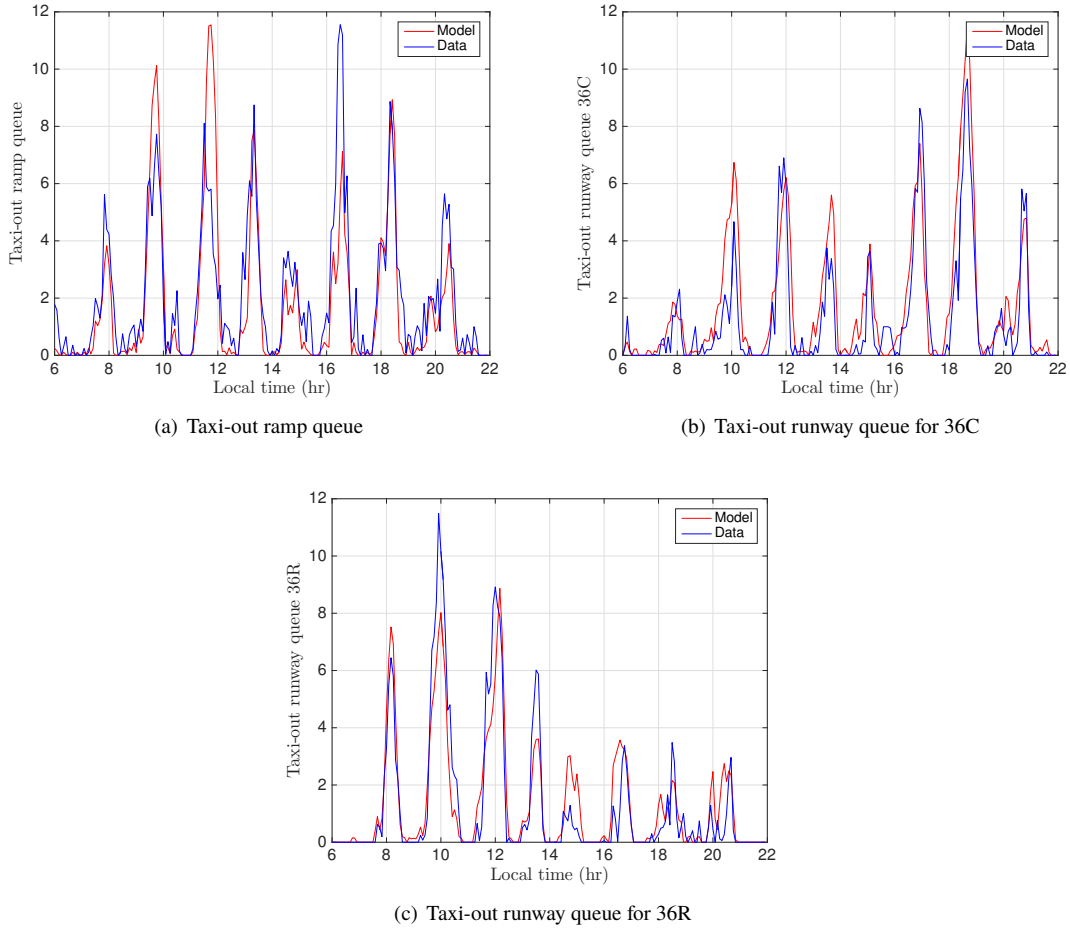


Fig. 3 Queue length predictions for taxi-out ramp and runway queue for a typical day (Jun 25, 2016).

time. The mean error for taxi-out time is -1.45 min, the mean absolute error (MAE) is less than 5 min for 69% of the flights. Also, errors in the gate to spot time prediction is larger when compared to spot to runway time prediction. This is expected since there is more unpredictability in the ramp area. One can get a sense of the magnitude of errors by comparing against the mean value of the actual taxi-out time. We had mentioned earlier that error in queue length prediction leads to error in taxi-time prediction. Another reason for errors in taxi-time prediction is because of the first-in-first-out assumption. In reality, the sequence of flights pushing back at the gate is not the same as the sequence of flights taking-off because of different routes and distances to the runway. Even a single flip in the sequence will lead to a taxi-out time error of more than a minute (which is the separation time between takeoffs at the runway). Although this might not show up in the mean error, it makes a difference when we consider mean absolute error in taxi-time. Fig. 7(a) shows a comparison between the distribution of predicted taxi-out time and actual values. We see that the two distributions match well except for the right tail of the data, that corresponds to flights with high taxi-out time. This explains why the mean error in taxi-out time is slightly negative.

Table 2 shows the error statistics for taxi-in flights computed from 8,477 flights from the test set. The mean error for taxi-in time is -1.08 min, the mean absolute error (MAE) is 3.82 min and MAE is less than 5 min for 78% of the flights. By comparing with the mean taxi-in time values we notice that the taxi-in time prediction has a higher relative mean error when compared to taxi-out time prediction. A significant contributor to the taxi-in time error is from the ramp portion. Fig. 7(b) shows a comparison between the distribution of predicted taxi-in time and actual values. Similar to taxi-out time, we see that the two distributions match well except for the right tail of the data, that corresponds to flights with high taxi-in time.

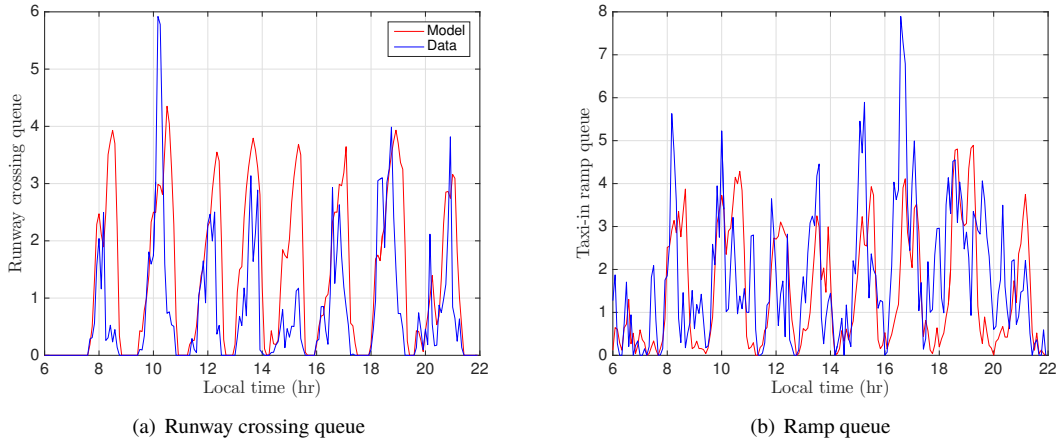


Fig. 4 Queue length predictions for taxi-in ramp and runway crossing queue for a typical day (Jun 25, 2016)

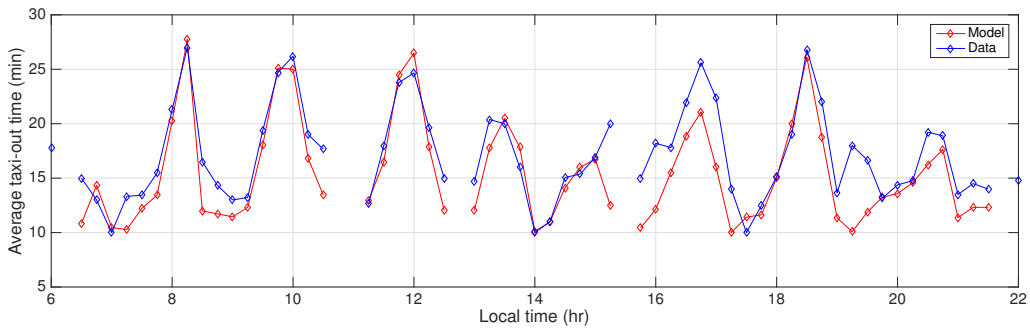


Fig. 5 Taxi-out time averaged over 15 min interval for a typical day (Jun 25, 2016).

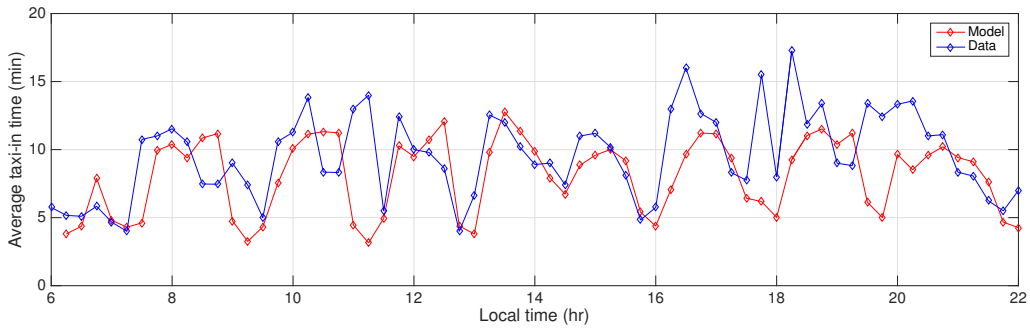


Fig. 6 Taxi-in time averaged over 15 min interval for a typical day (Jun 25, 2016).

Statistic (min)	Gate to spot	Spot to runway	Taxi-out
Mean values	9.68	10.40	20.09
Mean error	-0.87	-0.58	-1.45
Mean error	3.08	2.7	4.35
RMSE	3.78	3.9	4.41
Fraction of flights with error < 5 mins	0.82	0.86	0.69

Table 1 Error statistics for the taxi-out time based on 7,484 departure flights from the test set.

Statistic (min)	Runway to spot	Spot to gate	Taxi-in
Mean value	4.49	6.06	10.55
Mean error	-0.09	-0.99	-1.08
Mean error	1.38	3.34	3.82
RMSE	2.36	5.55	6.03
Fraction of flights with error < 5 mins	0.96	0.83	0.78

Table 2 Error statistics for the taxi-in time based on 8,477 arrival flights from the test set.

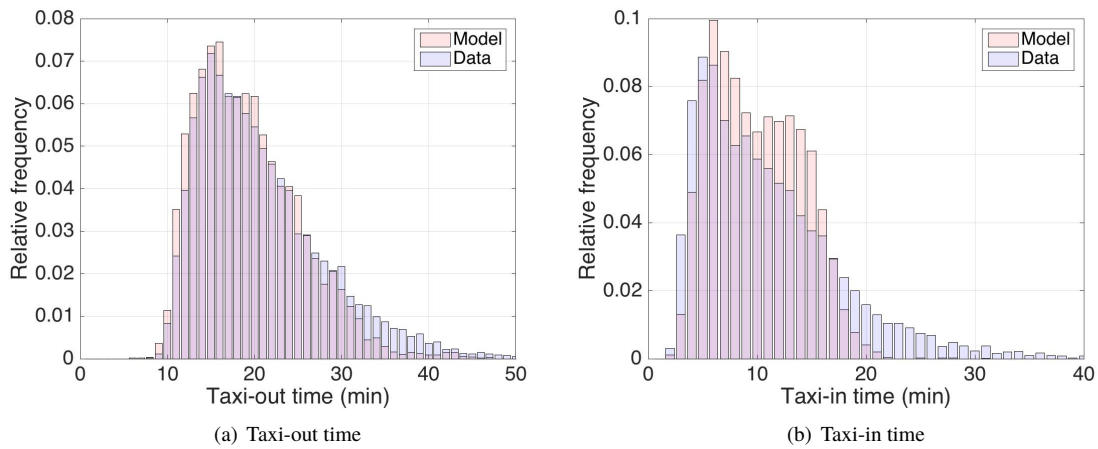


Fig. 7 Comparison of taxi-time distribution between the model and actual data from the test set.

IV. Departure metering

During periods when demand exceeds runway capacity, queues build up on the airport surface, leading to an increase in taxi-out time. This results in increased fuel burn which has both economic and environmental impact. Departure metering has been demonstrated to reduce the taxi-out time, leading to savings in fuel [5]. The idea behind departure metering is to hold flights at the gate when there are large queues on the airport surface and release them at the right time so that flights pass through smaller queues while taxiing. Departure metering is an integral part of FAA’s Terminal Flight Data Manager (TFDM), which is a NextGen initiative that is scheduled to be deployed from 2020 [20]. Many algorithms have been proposed to decide on the appropriate hold time at the gate [5–7, 10]. In this paper, we compute the metering benefits using NASA’s ATD-2 logic [21]. The ATD-2 logic for metering is a heuristic that computes a gate hold time based on predicted taxi-out time for each flight. NASA has been performing field trials at CLT since November 2017 to assess the benefits of using this logic for departure metering. The ATD-2 logic for departure metering is as follows,

$$TOBT = \max(EOBT, TTOT - X * UTT - Y) \tag{23}$$

Here, $TOBT$ is the Target Off Block Time or the new gate release time decided by the controllers, $TTOT$ is the Target Take Off Time, UTT is the Unimpeded Time to Take-off for each gate-runway pair, X is a constant factor, Y is the excess queue time buffer. The target take-off time is computed by adding the predicted taxi-out time to the flight’s EOBT ($TTOT = EOBT + T_{out}$). In this paper, we use the queuing model presented earlier to obtain the taxi-out time prediction for each flight. We also consider X to be unity. Essentially, the hold time assigned to each flight is $\max(0, T_{out} - UTT - Y)$. Note that $T_{out} - UTT$ represents the predicted excess time that an aircraft would unnecessarily spend waiting on the airport surface. The idea is to transfer the excess queue time to hold time at the gate, resulting in fuel savings. In addition, an excess queue time buffer (Y) is subtracted to account for errors in taxi-out time prediction.

A. Simulation environment for departure metering analysis

The metering algorithm is tested using a stochastic simulation of the airport surface. The simulator is a discrete queuing network model for the airport shown earlier in Fig.1(b) with the service time of each server being sampled from an empirical distribution. The empirical service time distributions are a function of the airport traffic such as number of landings on the runway and traffic on the ramp as discussed earlier. The key difference when compared with the analytical queue model is that service times are random and the simulations are repeated multiple times to obtain consistent statistics (a Monte-Carlo simulation with 20 runs). For the departure metering analysis, we consider a 15 day period that has 6,447 departures and 7,158 arrivals. Table 3 shows the error statistics for the simulator by comparing it with the actual data.

In this section, we assume that we have accurate EOBT information, *i.e.* the estimate of the push-ready time published by the airlines is accurate. We will ignore this assumption in the next section where we will account for errors in the EOBT information. In the field tests conducted by NASA at CLT, the hold time is assigned to flights when the pilot calls ready. However, in the future, the plan is to assign gate holds several minutes prior to the flight’s EOBT to improve predictability in the system. Let T_p be the planning horizon, which is the duration before a flight’s EOBT that a hold decision is made. At time T_p prior to a flight’s EOBT, the taxi-out time for a flight is predicted from the analytical queue model using the current state of the airport as the input. The gate release time (TOBT) for the flight is then determined using eq. 23. The flights are released at TOBT in the discrete queuing simulation of the airport.

Statistic	Gate to spot time	Spot to take-off time	Taxi-out time	Taxi-in time
Mean error (min)	-0.25	1.36	1.11	0.39
Mean error (min)	3.04	3.13	4.62	4.24
RMSE (min)	4.29	4.33	6.15	6.12
Fraction of flights with error < 5 mins	0.82	0.81	0.64	0.71

Table 3 Error statistics for the stochastic airport simulator obtained by comparing with the actual data for 6,447 departures and 7,158 arrivals over a period of 15 days.

B. Departure metering benefits

The simulation results for departure metering with a planning horizon of 20 min is discussed in this section. Fig. 8 shows the simulation results using the departure metering algorithm for a typical day for different excess queue time buffer values (Y). We see that the reduction in taxi-out time is correlated with the hold-time. A larger hold time is assigned during periods when the baseline taxi-out time is high. With increase in excess queue time buffer, average hold-time reduces, leading to lower benefits in terms of taxi-out time reduction. This shows that the excess queue time buffer is an important parameter that influences the taxi-out time reduction. Next, we present a methodology to pick the buffer parameter.

Fig. 9(a) shows the average hold time and taxi-out time reduction for different excess queue time buffers computed for 6,447 flights over a period of 15 days. With increase in buffer value, we see a drop in the hold-time as well as reduction in the taxi-out time. Note that the difference between the hold-time and taxi-out time reduction is equal to the change in wheels-off time (shown in Fig. 9(b)). A positive value of change in mean wheels-off time indicates that the runway is under-utilized. This situation corresponds to an aggressive strategy of holding flights at the gate, leading to a loss in runway throughput. We see that for smaller values of buffer size, the mean change in wheels-off time is positive, indicating under-utilization of the runway. For higher values of the buffer size, we see that the mean change in wheels-off time is close to zero. The value fluctuates around zero because of the stochastic nature of the simulation and we expect the value to converge to zero with increase in the number of sample runs of the simulation. For the analysis in this paper, we consider mean wheels-off time within ± 0.1 min to be equal to zero. The optimal excess queue time buffer is chosen such that a high taxi-out time reduction is obtained while satisfying zero change in mean wheels-off time (no loss in runway utilization). For the 20 min horizon considered here, we can see that the optimal excess queue time buffer is 7 min and the corresponding reduction in taxi-out time is 2.68 min.

Table 4 shows various metrics for different values of the excess queue time buffer. The fraction of flights held decreases with increase in excess queue time buffer as expected. It is important to note that the taxi-in time does not change with departure metering. However, one needs to note that we do not consider any gate conflicts in the simulation. A gate conflict occurs when an arriving flight needs to wait for the gate occupied by another aircraft that is supposed to depart. Since the mean hold time of flights that are held is 4.3 min (corresponding to optimal buffer size), we do not expect many gate conflicts to occur just because of metering. More analysis needs to be done to confirm this claim. The last column in the table shows the mean absolute displacement in wheels-off order, a statistic that can be considered as a measure of fairness. A fair metering policy should ensure that the take-off order remains the same. We can see that the displacement in wheels-off order is high for small buffer values when the hold-time is large and reduces as the buffer value is increased. In the algorithm for departure metering, the Target Take Off Time (TTOT) for a flight is predicted based on updated values of TOBT for flights that had an earlier EOBT. The consequence of this is that when two flights have similar EOBTs, the one that has an earlier EOBT might be held more than the other flight (even if the unimpeded times are the same for both the flights). We tested another version of metering algorithm where the TTOT for a flight is predicted based on EOBTs of earlier flights and not using updated values of their TOBT. The results were promising in terms of fairness, the mean absolute change in wheels-off order decreased from 1.2 to 0.5 (for the optimal buffer). However, benefits in terms of taxi-out time reduction decreased from 2.68 min to 2.1 min.

A comparison of the taxi-out time distribution obtained in the metering case with the baseline simulation is shown in Fig. 10(a). We can clearly see fewer flights with higher taxi-out time in the metering simulation when compared to the baseline. The number of active departures on the airport surface also reduces (Fig. 10(d)). The hold time distribution for flights that were assigned a non-zero hold is shown in Fig. 10(b). We can see that the maximum hold time is less than 20 min. We would like the maximum hold to be small enough such that it does not cause gate conflicts. Fig. 10(c) shows the distribution of the time spent by the aircraft on the surface after push-ready for the metering case (hold time + taxi-out time) and the baseline case (taxi-out time). We see that the two distributions closely match, which implies that the departure metering does not impact the total time spent by the aircraft on the surface (also indicates runway is not under-utilized).

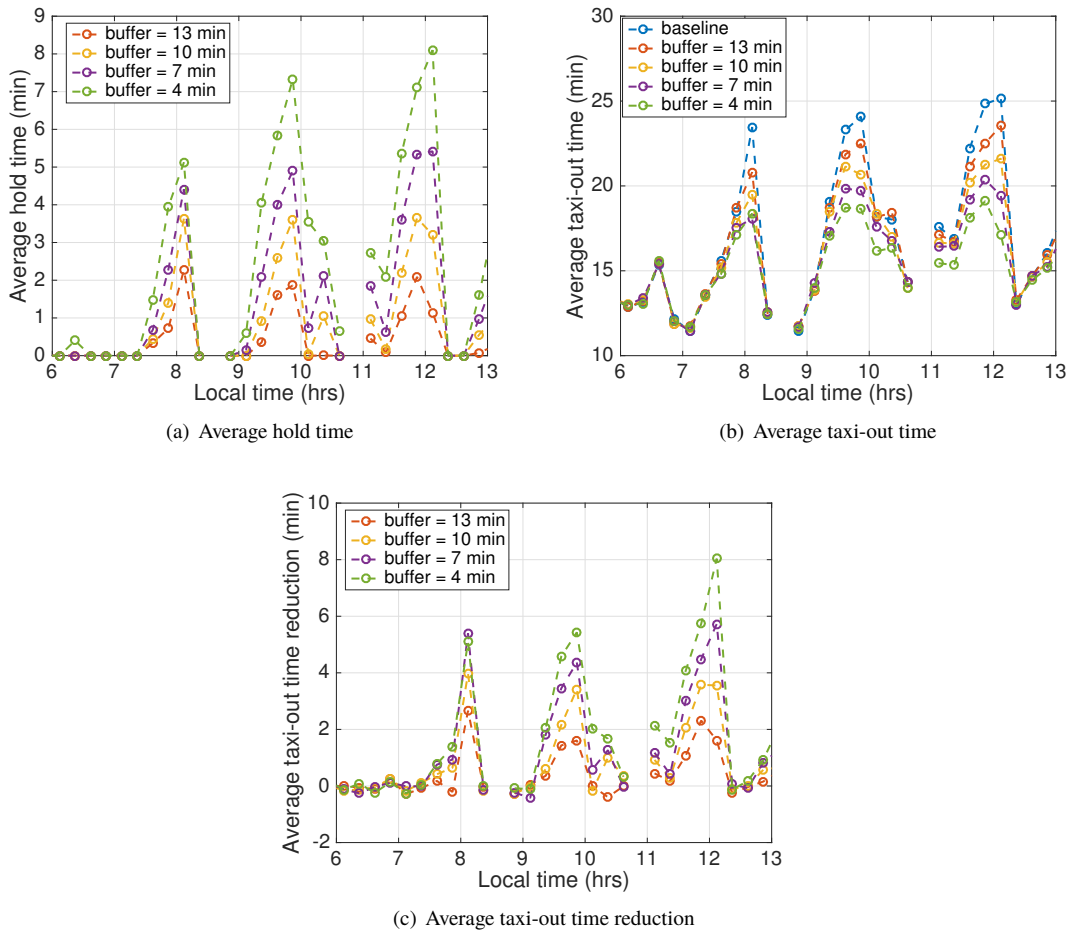


Fig. 8 Metering simulation results for different excess queue time buffer values. The plots show averaged values over a 15 min time window for a typical day (Jun 25th, 2016).

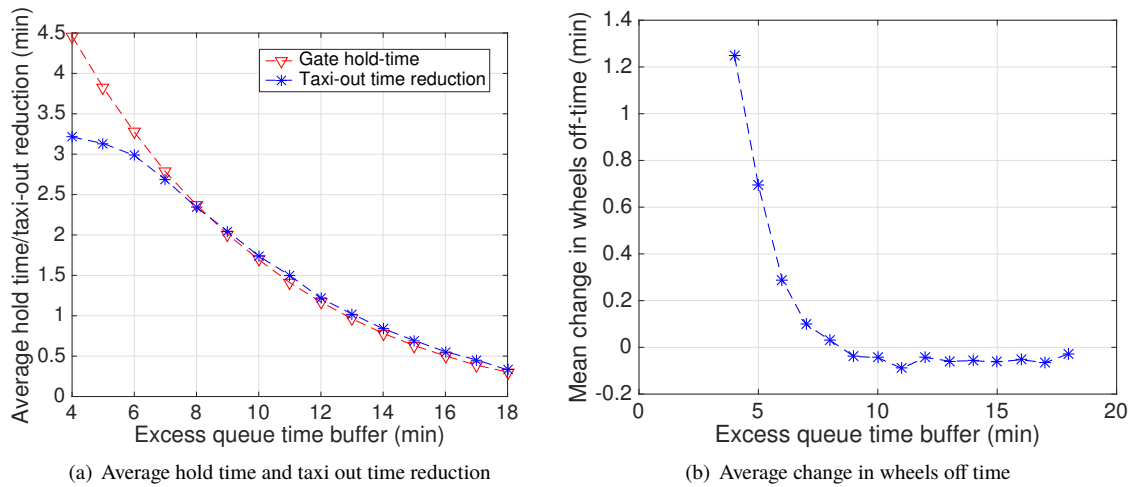
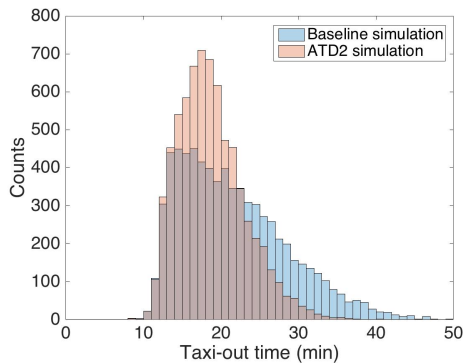


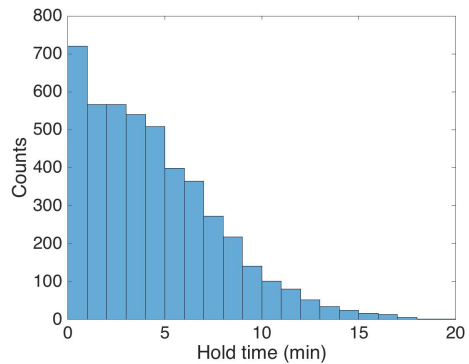
Fig. 9 Metering simulation results for different excess queue time buffer values for 6,447 departures over a period of 15 days.

Excess queue time buffer	Mean hold time over all flights	Fraction of flights held	Mean hold time of flights held	Fraction of flights held >2 min	Mean hold time of flights held >2 min	Mean taxi-out time reduction	Mean wheels-off time change	Mean taxi-in time reduction	Mean abs. change in wheels-off order
4	4.46	0.81	5.5	0.65	6.63	3.21	1.25	0	1.48
5	3.83	0.75	5.09	0.58	6.28	3.13	0.69	0.06	1.38
6	3.27	0.7	4.68	0.52	5.98	2.98	0.29	0.1	1.28
7	2.78	0.64	4.32	0.46	5.73	2.68	0.1	0.07	1.2
8	2.37	0.59	4.05	0.4	5.47	2.34	0.03	0.09	1.07
9	2.01	0.53	3.76	0.35	5.27	2.05	-0.04	0.08	0.95
10	1.7	0.49	3.49	0.29	5.18	1.74	-0.04	0.05	0.89
11	1.41	0.44	3.21	0.25	5.03	1.5	-0.09	0.06	0.77
12	1.17	0.39	2.99	0.21	4.87	1.21	-0.04	0.04	0.68

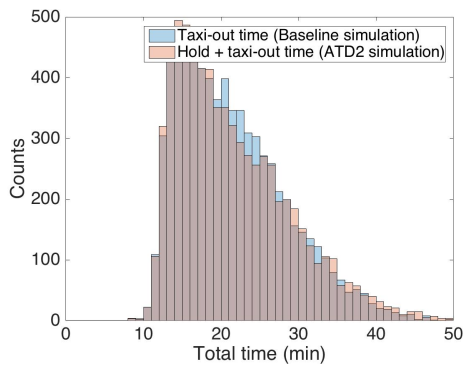
Table 4 Summary of metering benefits for different excess queue time buffer values. The units of time are in minutes.



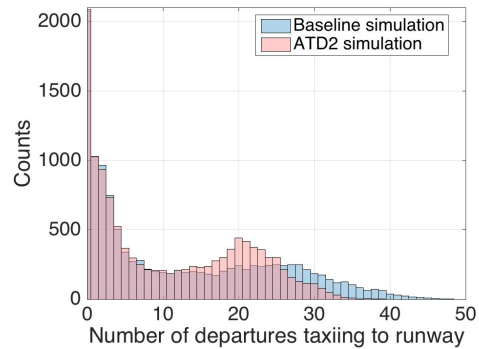
(a) Taxi-out time comparison



(b) Hold time distribution for the flights that were held



(c) Time on the airport surface after push-ready



(d) Number of active departures

Fig. 10 Distributions comparing departure metering with the baseline for a 20 min planning horizon with a optimal excess queue time buffer of 7 min.

V. Impact of EOBT uncertainty

The results for the taxi-out time prediction and departure metering presented earlier assumed that the expected push-ready time (EOBT information) provided by the airlines is accurate. However, the EOBT published by airlines often deviate from the actual push-ready time. Controllers need to make decisions based on the available EOBT information. This motivates us to study the impact of EOBT error on departure metering as well as on taxi-out time prediction.

A. EOBT uncertainty in airport operations

EOBT messages from the FAA's Traffic Flow Management System (TFMS) were evaluated for the flights of a major airline departing from CLT for the two month period beginning on December 13, 2017. During that period, 14,331 flights reported at least one EOBT message. Flights departing between 9am and 12pm (local) were removed to eliminate the effects of departure metering which occurred at CLT during this time period due to ATD-2 activities. For each EOBT message, the EOBT error was found by subtracting the Actual Off Block Time (AOBT) for that flight from the current EOBT. These errors were compared over different lookahead time horizons. The time horizon was determined by the difference between the time at which the EOBT message was transmitted and the current EOBT value. Each lookahead time step contained the EOBT messages that were transmitted since the previous time step, but limited to only the most recent message for each flight in case there were multiple EOBT messages for it within the time period being considered. This approach allows an assessment of the accuracy of the EOBT at different time horizons. Fig. 11 shows the results of fitting a Probability Density Function (PDF) to the distributions at 5, 10, 20, 30, 40, 50, 60 and 120 minutes lookahead time steps. The key statistics of these curves are presented in Table 5. It was expected that the standard deviations of the curves would increase with increasing lookahead time. This was observed for lookahead times less than 50 minutes, but not for the 60 and 120 minute lookahead curves. In addition, a significant reduction in the standard deviation of the curves was observed below 30 minutes compared to 30-50 minute lookahead times.

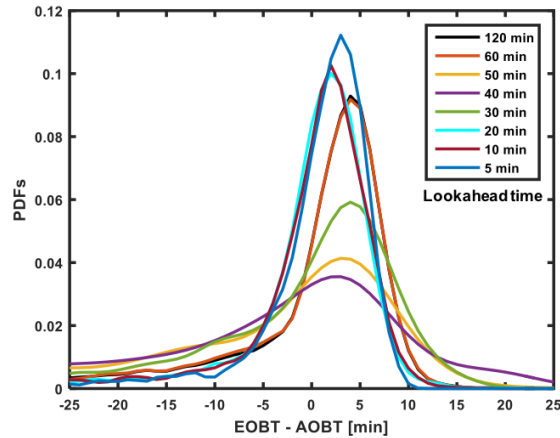


Fig. 11 Probability Distribution Functions (PDFs) of EOBT errors at CLT (12/13/17-2/12/18).

Lookahead time (min)	5	10	20	30	40	50	60	120
Mean error (min)	1.83	1.48	1.37	-0.07	-4.52	5.25	1.78	1.87
Median error (min)	2.35	1.8	1.7	2.22	0	0.93	3	3
Std. Dev. of error (min)	3.47	3.9	3.88	8.85	14.65	14.05	5.65	5.6

Table 5 EOBT error statistics for different lookahead times.

To explore these issues, Fig. 13 shows the differences between the Initial Gate Time of Departure (IGTD, defined as the original scheduled gate push back time for the flight) and the EOBT, for the same flights used in Fig. 11. For the distributions between 5-30 minutes lookahead time, there is some spread across the comparisons of IGTD and EOBT. However, beginning at approximately 40 minutes, there is a noticeable change where the majority of the EOBT and

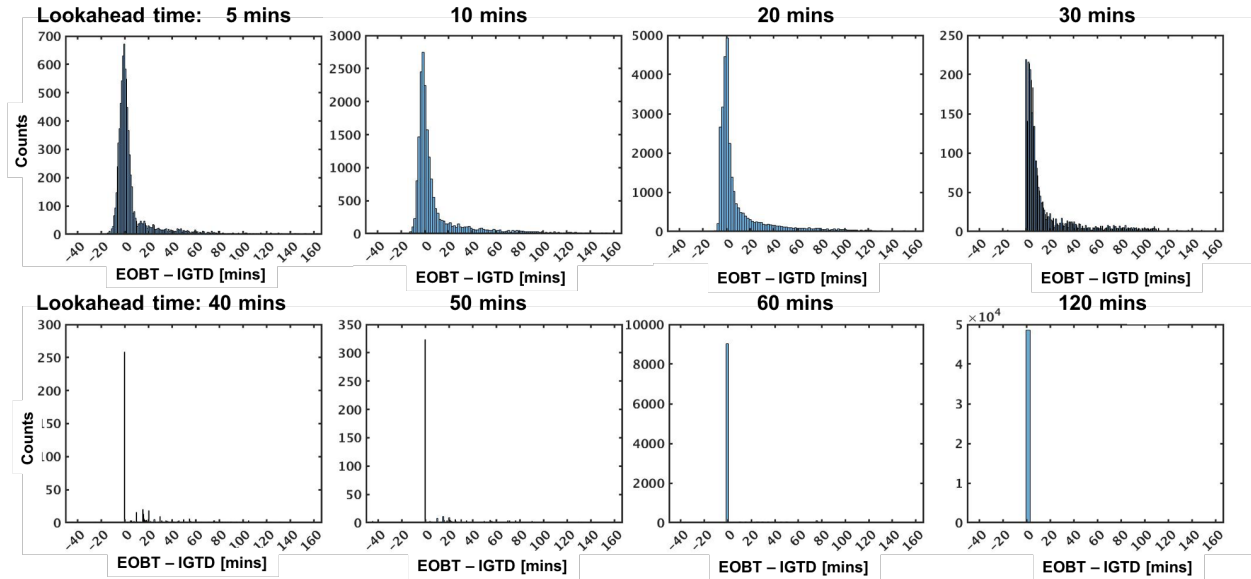


Fig. 12 IGTD and EOBT time comparisons at different lookahead times.

IGTD values are the same ($EOBT - IGTD = 0$), with this trend continuing with time steps that are further out until at 60 and 120 minute lookahead times when the EOBT and IGTD match almost identically. This indicates that, in this dataset, reported EOBTs are mostly using the IGTD until about 30 minutes before expected pushback.

These observations are driving some of the characteristics observed in the PDFs in Fig. 11. Fig. 14 depicts how close to the actual pushback time most of the EOBT messages are transmitted. This shows that the majority of the messages are published within 30 minutes of the actual pushback when the EOBT messages are mostly “real” updates instead of the IGTD value.

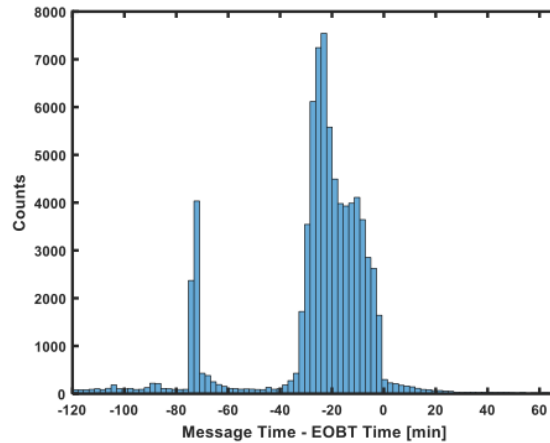


Fig. 13 Frequency of transmitted EOBT messages (within 2 hours)

Further work is required to fully understand why the EOBT values largely based on IGTD estimates at 60 minutes and out result in lower EOBT errors compared to 30-50 minute lookahead times. For now, in this analysis we are using only EOBT error characterizations based on lookahead times below 60 minutes to eliminate the impacts of IGTD data, and those subset of results are presented in Fig. 15.

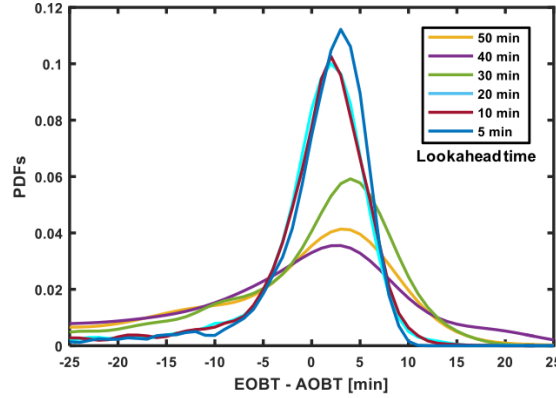


Fig. 14 Probability Distribution Functions (PDFs) of EOBT errors at CLT (12/13/17-2/12/18) using less than 60 minute lookahead times

B. Taxi-out time prediction with EOBT uncertainty

The taxi-out time predictions presented earlier needed the actual gate out time as the input for the analytical queue model. The accuracy of the predictions is expected to deteriorate with errors in the inputs. In this section, the impact of an inaccurate EOBT on taxi-time prediction is investigated through a parametric analysis. For the analysis, we assume that the EOBT error distributions are Gaussian with a zero mean and varying standard deviation over a range consistent with the empirical EOBT uncertainty results presented above. We adopt this methodology instead of using the actual distribution since it allows us to investigate the impact of different error distributions in a systematic way. The range of the parametric space for the standard deviation of the error distribution follows from the operational data. The EOBT time is synthetically computed for every flight in the data-set by using the Actual Off Block Time (AOBT) and a sample of the EOBT error distribution ($EOBT = \text{error} + AOBT$). We use the EOBT time as the input in the analytical queue model to predict the taxi-time and compare the results with the actual data in which flights pushed back at the AOBT time. Fig. 16(a) shows the mean absolute prediction error for the taxi-out time as a function of the standard deviation of the EOBT error. Standard deviation value of zero indicates that there is no uncertainty, *i.e.* the EOBT corresponds to the actual out-gate time. We can see that the magnitude of the prediction error increases with increase in uncertainty of EOBT information. The mean prediction error (Fig. 16(a)) increases in the negative sense for higher uncertainty in EOBT, which implies that the taxi-out time is under-predicted with EOBT uncertainty. This can also be seen in the error distributions for predicted taxi-out time shown in Fig. 17(a). The peak value of the distribution shifts to the left away from zero with increase in standard deviation of the EOBT error. The width of the error distribution slightly increases which we can notice from the drop in the peak value. The reason why the taxi-out time is under-predicted can be attributed to the change in the demand profile of predicted number of aircraft that are ready to push-back. Fig. 16(b) shows the predicted demand profile obtained from EOBT for different EOBT error distributions. We see that the peak value in the predicted gate demand drops and the demand is more 'smoothed-out' as the standard deviation of the EOBT error increases. Lower peak demand leads to under-prediction of the taxi-out time, resulting in the mean error to be more negative.

C. Departure metering benefits with EOBT uncertainty

The EOBT uncertainty impacts departure metering for two reasons: (a) reduced prediction accuracy of taxi-out time and (b) non-compliance with the assigned TOBT time. In reality, the actual push-ready time is different from the EOBT time published by the airline, leading to an inefficient hold-time assignment. Similar to the earlier analysis, we assume that the EOBT error distribution is Gaussian with zero mean and vary the standard deviation over the same range informed by the empirical EOBT uncertainty results.

First, let us take a closer look at NASA's ATD-2 logic for departure metering (eq. 23) in the presence of EOBT error. Depending on the push-ready time, we can have the following three cases,

- Case (a) push-ready time < EOBT: The metering logic suggests that the flight needs to hold until the EOBT time even if the predicted excess queue time (along with the buffer) is equal to zero. This strategy improves predictability in the system since flights are required to push-back at the EOBT time, but flights have to unnecessarily hold at

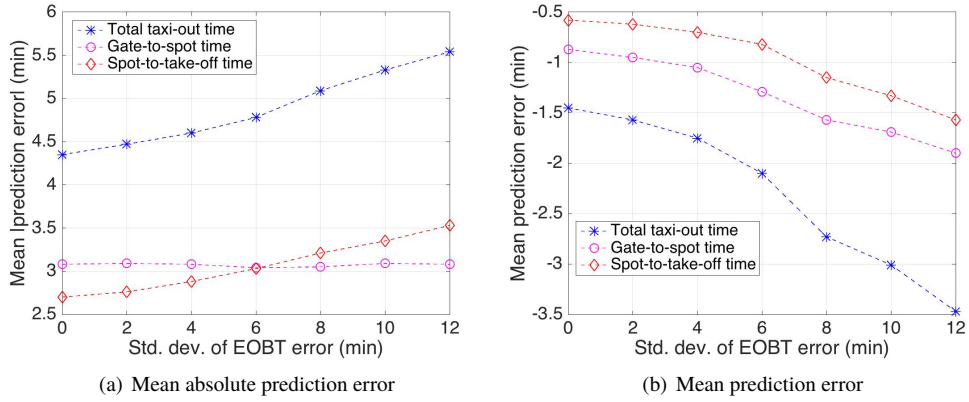


Fig. 15 Error in predicted taxi-out time for various EOBT error distributions for 7,484 flights in the test set.

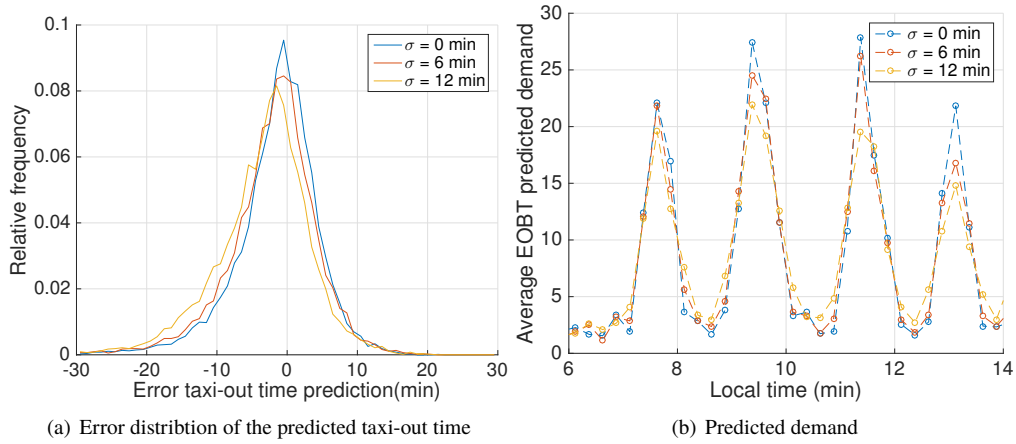


Fig. 16 (a) Error distribution for the predicted taxi-out time for different standard deviation values of the EOBT error distribution (b) A 15-min-average predicted out-gate demand based on EOBT with different standard deviation values of the error distribution.

the gate which might cause a loss in runway throughput.

- Case (b) $EOBT \leq \text{push-ready time} \leq TOBT$: There are no issues in this case since the flight waits and then pushback happens at TOBT.
- Case (c) $TOBT < \text{push-ready time}$: The flight pushback happens after the assigned TOBT time. Similar to the first case, we lose predictability and there might be a loss in runway throughput because the flight did not pushback when it was supposed to.

To prevent unnecessary holds in Case (a), we modify the metering logic to let flights pushback at the push-ready time if the predicted excess queue time (along with the buffer) is equal to zero. Although we lose predictability, we get better runway utilization. Fig. 18(a) shows the average hold time and taxi-out time reduction for various excess queue time buffer values using the metering algorithm with EOBT uncertainty. We see that the hold time is greater than the taxi-out time reduction for all the buffer values, indicating a loss in runway utilization. A similar plot is shown in Fig. 18(b) for the modified version of the algorithm where flights are allowed to push-back at the push-ready time if the predicted excess queue time (along with the buffer) is equal to zero. We see that for buffer parameter greater than 10 min, the hold time is equal to the taxi-out time reduction, which implies no loss in runway utilization. This shows that the modified version of the algorithm performs better and further results in this paper will be presented based on this modification.

For each value of standard deviation of the EOBT error distribution, the optimal buffer size is determined. The optimal excess queue buffer is the smallest value of the queue buffer for which the mean change in off-time is equal to

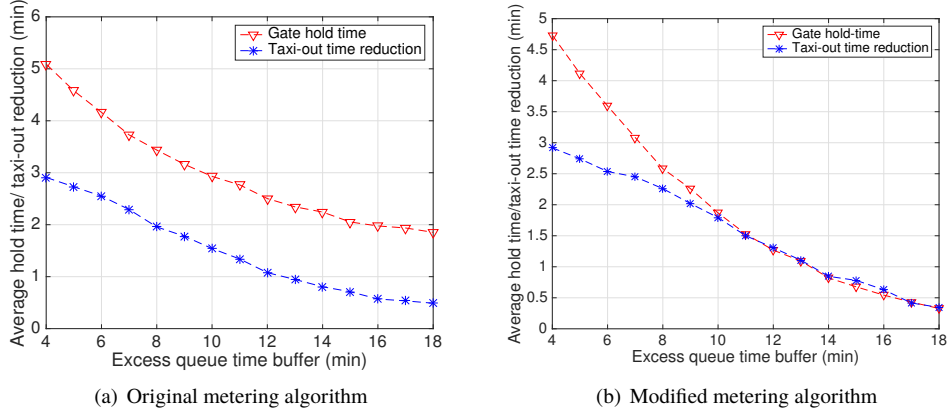


Fig. 17 Average hold time and taxi-out time reduction as a function of excess queue time buffer with a 4 min standard deviation in EOBT error.

zero. Fig. 19(a) shows the optimal excess queue buffer time for different EOBT distributions and two different planning horizons (10 min and 20 min). For a particular planning horizon, the optimal buffer time increases with increase in EOBT error and then saturates beyond a particular point. The increase in buffer time is expected since the taxi-out time prediction error increases with EOBT uncertainty and we need to compensate for that with a higher excess queue time buffer. We also notice that for higher EOBT errors, a larger buffer size is required for the 20 min planning horizon when compared to the 10 min horizon. The predictive performance of the model deteriorates with increase in time horizon, so it is natural to expect the 20 min horizon to have a higher buffer value. The reason as to why we do not see a larger buffer size at lower EOBT errors could be because the parametric analysis to determine the optimal excess queue time was done at a discretization level of 1 min and anything smaller than 1 min would not show up in the analysis. This might also be the reason for the curves to saturate since increase in the optimal buffer value beyond a particular point might be smaller than the discretization level.

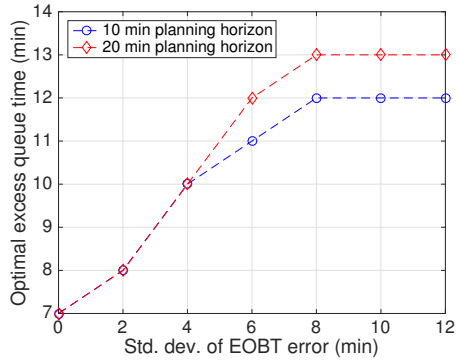
Next, we present some metrics to analyse departure metering benefits for different EOBT error distributions using the optimal excess queue buffer time. The benefits in terms of taxi-out time reduction decreases with increase in EOBT error as seen in Fig. 19(b). We see lower benefits for the 20 min time horizon when compared to the 10 min time horizon. The taxi-out time benefits depends on the hold time when we are using the optimal buffer (since there is no loss in runway throughput). Since we have higher excess queue time buffers for higher EOBT errors, the average hold time (Fig. 19(c)) and the number of flights held decreases (Fig. 19(e)), resulting in a smaller reduction in taxi-out time. But it is interesting to note that the mean hold time of the flights that were assigned a positive hold increases with EOBT uncertainty (Fig. 19(d)). The mean absolute displacement in wheels-off order is shown in Fig. 19(f). We see an initial increase and then a drop in its value. We can attribute the initial increase to the EOBT error and the drop later on because of the decrease in the number of holds.

The analysis quantifies the benefits that the airlines can have by publishing more accurate EOBTs in terms of taxi-out time reduction. In the current operations, the standard deviation of the EOBT error distribution is around 4 min for a 20 min time horizon (Table 5). If the airlines improve the EOBT accuracy by reducing the standard deviation of the error by half to 2 min, the benefits in terms of taxi-out time reduction increases by 25.7%. This improvement should encourage airlines to publish better EOBT information.

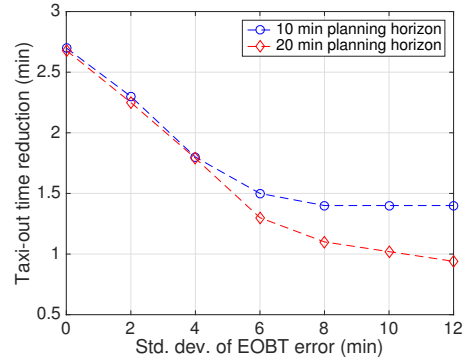
VI. Conclusions and future work

The highlight of the model presented in this paper is that it is able to combine arrival and departure operations, and provide a set of equations that can be used to predict the queue length at key congestion areas on the airport surface. The analytical queue model requires integrating a few equations forward in time which is computationally efficient when compared to a discrete event simulation. Using the queue length information, one can predict the taxi-times for arrivals as well as departures.

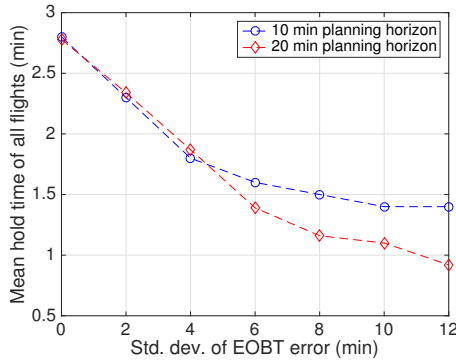
The metering benefits in terms of taxi-out time reduction was obtained using NASA's ATD-2 logic with the help of predictions from the queue model. A methodology was proposed to estimate the optimal value of the excess queue time



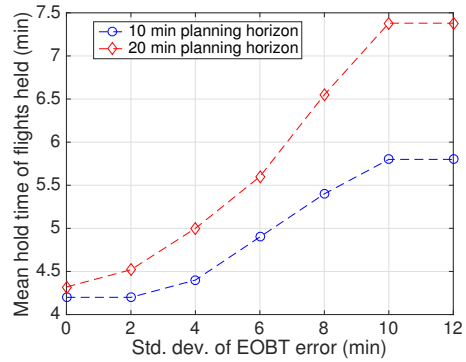
(a) Optimal excess queue time buffer



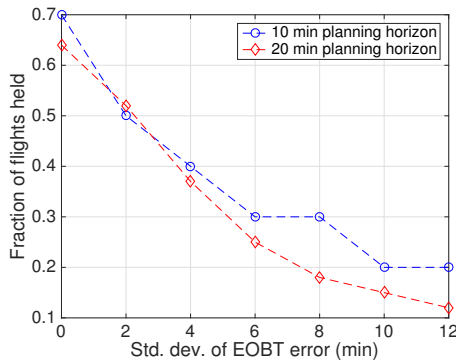
(b) Taxi-out time reduction



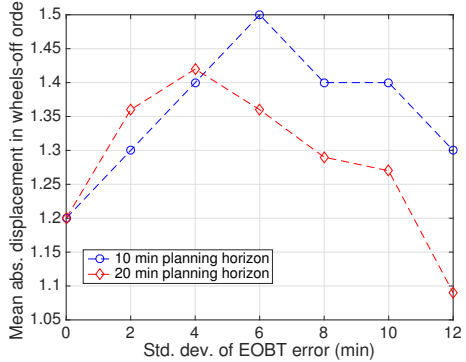
(c) Mean hold time



(d) Mean hold time of the flights that are held



(e) Fraction of flights held



(f) Mean absolute displacement in wheels-off order

Fig. 18 Departure metering analysis for two planning horizons and different standard deviation values of the EOBT error distribution.

buffer which is an important parameter that dictates the benefits. In the field tests at CLT [22], an excess queue time buffer of around 10 min is currently used which is slightly higher compared to our optimal estimate of 7 min when there is no EOBT uncertainty. This shows that the controllers might be slightly conservative in terms of holding flights and are obtaining lower benefits than what is potentially possible. However, there are other factors that influence the buffer size such as the accuracy of the taxi-out time prediction which might be different compared to the model presented in this paper.

Another important contribution of this paper is that we have presented empirical results of current EOBT uncertainty at CLT and have also provided an empirical relationship between EOBT uncertainty and taxi-out time savings. We showed that there is a need to have a larger excess queue time buffer depending on the EOBT uncertainty and planning horizon. This resulted in lower benefits in terms of taxi-out time reduction. We could further estimate savings in fuel consumption from the reduction in taxi-out time. The fuel and cost savings should incentivize airlines to publish more accurate EOBTs. In the future, instead of using synthetic EOBT values, we plan to use the actual EOBT time from data and compute the reduction in benefits.

A promising direction for future work is to look at ways of preventing airlines from manipulating the system by publishing inaccurate EOBTs to obtain more benefits. If an airline can guess the amount of hold that it could receive, it can report an earlier EOBT so that the assigned TOBT by the controllers would be close to the actual push-ready time, leading to improved benefits for the airline in terms of delay reduction. To prevent such gaming, we might need to develop a strategy-proof mechanism such that airlines do not gain any benefits by reporting inaccurate EOBTs. The other interesting question in the case of multiple airlines is the following: does an airline that published more accurate EOBT information end up with more benefits or is the benefit enjoyed by other airlines? To incentivize airlines to publish more accurate EOBTs, NASA plans to categorize flights into planning group and uncertain group based on the historical accuracy of their EOBT information. The idea is to give priority to the flights in the planning group so that they are able to get more benefits. There are many challenges even with this approach (a) deciding on a criterion to categorize flights into two groups (airlines could game by reporting accurate EOBTs during periods with less congestion and incorrect EOBTs during periods with congestion to obtain more benefits) and (b) developing strategies to penalize the uncertain group.

In this paper, the uncertainties in EOBT and taxi-time prediction were handled by modifying the excess queue parameter in the metering logic. However, we could explore concepts from robust control theory to determine an algorithm that explicitly accounts for these uncertainties with theoretical guarantees. In addition to assigning hold time at the gate, another important decision that will influence the taxi-out time is the runway assignment. In the current operations at CLT, during periods of congestion, we see significant differences in the taxi-out time between the two runways. An algorithm that can optimally decide the runway assignment as well as hold time is expected to yield more benefits. The other possible uncertainty that would impact operations is the error in the predicted arrival rate. We have assumed accurate information of the landing time for the arrivals into the future to estimate the runway capacity for the departures. Although this is known to some degree of accuracy, it is interesting to investigate the impact of arrival rate uncertainty as well.

VII. Acknowledgements

The authors would like to thank the ATD-2 Remote Demo team at NASA (Shivanjli Sharma, Yoon Jung, Jeremy Coupe, Leonard Bagasol, Isaac Robeson, Liang Chen, Hanbong Lee and others) for providing information about the ongoing departure metering field trials at CLT. Many thanks to Christopher Dorbian of the FAA Office of Environment and Energy for his support of this activity.

References

- [1] International Air Transport Association (IATA), “Industry Facts and Statistics,” 2017. [Http://www.iata.org/](http://www.iata.org/).
- [2] ACRP, “Methodology to Improve AEDT Quantification of Aircraft Taxi/Idle Emissions,” 2016.
- [3] Khadilkar, H., and Balakrishnan, H., “Estimation of aircraft taxi fuel burn using flight data recorder archives,” *Transportation Research Part D: Transport and Environment*, Vol. 17, No. 7, 2012, pp. 532–537.
- [4] Federal Aviation Administration (FAA), “Aviation Environmental Design Tool (AEDT),” 2017. [Https://aedt.faa.gov](https://aedt.faa.gov).
- [5] Simaiakis, I., Khadilkar, H., Balakrishnan, H., Reynolds, T. G., and Hansman, R. J., “Demonstration of reduced airport congestion through pushback rate control,” *Transportation Research Part A: Policy and Practice*, Vol. 66, 2014, pp. 251–267.

- [6] Pujet, N., Delcaire, B., and Feron, E., "Input-output modeling and control of the departure process of busy airports," *Air Traffic Control Quarterly*, Vol. 8, No. 1, 2000, pp. 1–32.
- [7] Badrinath, S., and Balakrishnan, H., "Control of a non-stationary tandem queue model of the airport surface," *American Control Conference (ACC), 2017*, IEEE, 2017, pp. 655–661.
- [8] Aponso, B., Coppenbarger, R., Jung, Y., Quon, L., Lohr, G., and O'Connor, N., "Identifying Key Issues and Potential solutions for Integrated Arrival, Departure, Surface Operations by Surveying Stakeholder Preferences," *15th AIAA Aviation Technology, Integration, and Operations Conference*, 2015.
- [9] Simaiakis, I., and Pyrgiotis, N., "An analytical queuing model of airport departure processes for taxi out time prediction," *AIAA Aviation Technology, Integration and Operations (ATIO) Conference*, 2010.
- [10] Khadilkar, H. D., "Networked control of aircraft operations at airports and in terminal areas," Ph.D. thesis, Massachusetts Institute of Technology, 2013.
- [11] Windhorst, R. D., Montoya, J. V., Zhu, Z., Gridnev, S., Griffin, K., Saraf, A., and Stroiney, S., "Validation of simulations of airport surface traffic with the surface operations simulator and scheduler," *Los Angeles, CA, 13th AIAA Aviation Technology, Integration, and Operations Conference*, 2013.
- [12] Lee, H., Malik, W., Zhang, B., Nagarajan, B., and Jung, Y. C., "Taxi time prediction at Charlotte Airport using fast-time simulation and machine learning techniques," *15th AIAA Aviation Technology, Integration, and Operation (ATIO) Conference, Dallas, TX*, 2015.
- [13] McFarlane, P., and Balakrishnan, H., "Optimal control of airport pushbacks in the presence of uncertainties," *American Control Conference (ACC), 2016*, IEEE, 2016, pp. 233–239.
- [14] OAG, "Charlotte airport operations data," , 2015.
- [15] Simaiakis, I., Sandberg, M., and Balakrishnan, H., "Dynamic control of airport departures: Algorithm development and field evaluation," *IEEE Transactions on Intelligent Transportation Systems*, Vol. 15, No. 1, 2014, pp. 285–295.
- [16] Wang, W.-P., Tipper, D., and Banerjee, S., "A simple approximation for modeling nonstationary queues," *INFOCOM'96. Fifteenth Annual Joint Conference of the IEEE Computer Societies. Networking the Next Generation. Proceedings IEEE*, Vol. 1, IEEE, 1996, pp. 255–262.
- [17] Tipper, D., and Sundareshan, M. K., "Numerical methods for modeling computer networks under nonstationary conditions," *IEEE Journal on Selected Areas in Communications*, Vol. 8, No. 9, 1990, pp. 1682–1695.
- [18] *ASDE-X brochure - ASDE-X 10/05.qxd*, Sensis Corporation, East Syracuse, NY, 2008.
- [19] Federal Aviation Administration (FAA), "Aviation System Performance Metrics (ASPM) website," , 2017. [Http://aspm.faa.gov/](http://aspm.faa.gov/).
- [20] Federal Aviation Administration (FAA), "TFDM Overview," , 2018. [Https://www.faa.gov/](https://www.faa.gov/).
- [21] NASA Remote Demos, "Tactical Surface Metering Briefing," , 2018. [Https://www.aviationsystemsdivision.arc.nasa.gov/](https://www.aviationsystemsdivision.arc.nasa.gov/).
- [22] NASA Remote Demos, "Surface Metering - Initial Analysis, Impact, and Evolution," , 2018. [Https://www.aviationsystemsdivision.arc.nasa.gov/](https://www.aviationsystemsdivision.arc.nasa.gov/).